Design Trade-offs of Wind Turbine Preview Control

Ahmet Arda Ozdemir, Peter Seiler, *Member*, IEEE, and Gary J. Balas, *Fellow, IEEE*

***Abstract*—Recent work has demonstrated the benefits of preview wind measurements for turbine control. This paper investigates the basic design trade-offs between turbine performance, preview time, and pitch actuator rate limits. A Region 3 rotor-speed tracking problem is formulated in continuous-time as an optimal control problem using a simple one-state rigid body turbine model. The exact, analytical solution to this problem provides insight into the fundamental performance limits. These analytical results are compared with the performance of an H_∞ preview controller simulated on a higher fidelity, nonlinear turbine model with realistic wind sensor models. The performance versus preview time characteristics of the H_∞ controllers are in agreement with the predictions from the lower fidelity model. Thus the analytical results obtained with the low-order model can provide design guidelines for the use of preview information in turbine control.**

***Index Terms*—Wind Turbines, Preview Control**

I. Introduction

THE economics of wind energy has driven the wind industry to turbines of enormous sizes. However, this increase in size comes with higher structural flexibility and loads. The design of turbine blades, tower, generator and balancing structures are often limited by these increased load requirements. Naturally, the use of controls for turbine structural load reduction has been a popular topic in literature [1], [2].

Wind speed fluctuations play a key role in the structural loads incurred in wind turbines. Current turbines use anemometers mounted on the rear of the nacelle for wind speed measurements. However, these anemometers measure a disturbed wind field since they are located behind the turbine rotor. The low quality anemometer measurements are typically not used for closed-loop control. Alternatively, recent work in the turbine control literature has focused on the use of advanced sensors, e.g. LIDARs, to measure the incoming wind field [3]–[8]. These sensors can be mounted on the rotor hub in a forward looking fashion. This setup offers three key benefits. First, a higher accuracy measurement of the undisturbed wind field can be obtained. Second, spatial variations in the wind field can be detected. Lastly, wind fluctuations are detected before their impact on the turbine. Turbine control systems can be designed to utilize this information and minimize the impact of wind speed variations.

Various methodologies have been studied for turbine preview control. Reference [4] investigates pitch rate constrained H_∞ preview controllers designed via linear matrix inequality methods. The maximum singular value of these full-information H_∞ controllers are presented for various preview times and pitch rate limitations. These preview controllers are simulated on a high-fidelity turbine model with ideal and noisy preview measurements. The load reduction performance is deteriorated with noisy measurements while ideal measurements yielded improved results compared to a baseline non-preview controller. References [5]–[7] investigate model predictive control (MPC) methods. [5] focuses on blade load reduction while avoiding generator over-speed. MPC controllers with 0.45 and 1 s of preview are shown to improve load reduction performance both with ideal as well as noisy preview measurements on high-fidelity models. [6] compares linear time-invariant, linear parameter-varying (LPV) and nonlinear MPC formulations. Reference [7] uses an LPV MPC formulation with an optimal wind estimator. Comparison of the LPV MPC controller to a traditional PID controller showed an 80% reduction in peak tower and gearbox loads for a 50-year extreme gust condition. Model inversion techniques and the use of genetic algorithms for preview controllers were investigated in [8]. These are designed as separate feedforward controllers to be operating simultaneously with more traditional feedback control laws. The model inversion methods were found to decrease blade loads at the expense of increasing tower loads. Finite impulse response filters tuned by genetic algorithms were found to improve both blade and tower loads with minimal increase in control effort [8]. In summary, all these control design methods rely on numerical studies to investigate the impact of different sensor models and additional preview time. The resulting controllers are tested with Monte Carlo simulations on high fidelity, nonlinear turbine models to understand the impact of preview time. These studies provide useful insight about the effects of additional preview information. However, all the approaches depend on specific design choices, e.g. the control methodology and design weights.

This paper aims to understand the fundamental trade-offs between performance, wind preview time, and blade pitch rate limits. The objective is to use preview information to reject wind disturbances subject to blade pitch rate constraints. A Region 3 rotor speed regulation problem is studied using two different fidelity models. First, an optimal control problem is formulated in continuous-time for a simple one-state, linear rigid-body model of a wind turbine. The exact, analytical solution of this problem provides insight into the fundamental performance limits. Second, H_∞ preview controllers are designed for a number of preview times. These controllers are simulated on a higher fidelity, nonlinear turbine model with realistic preview sensor models. The performance versus preview time characteristics of the H_∞ controllers are in agreement with the predictions from the lower fidelity models. Thus we believe the analytical results obtained with the low-order model can provide design guidelines for the use of

A. Ozdemir, P. Seiler and G. J. Balas are with the Department of Aerospace Engineering and Mechanics, University of Minnesota, Minneapolis, MN, 55455 USA e-mail: (arda,seiler,balas)@aem.umn.edu.

preview information in turbine control.

This paper extends our previous work contained in the papers [9] and [10]. Our earlier work in [10] investigates performance limits of turbine preview control via numerical solutions of linear programs. Reference [9] derives the analytical solution for preview control of first order systems with actuator rate constraints. A simplified version of these results is presented here to gain insight into the wind turbine preview control problem. The performance versus preview time trends predicted by these results are validated with high-fidelity turbine models with advanced controllers. A sensor model that captures the error characteristics of a common LIDAR wind sensor is implemented to investigate the preview wind sensing challenges. The sensitivity of the results to the changes in the operating condition is also investigated.

The remainder of the paper is structured as follows: Sections II and III discuss, in order, the results for the simple one-state model and the higher fidelity nonlinear model of the turbine. Section III also discusses the challenges associated with the preview wind measurements. Section IV compares the preview versus performance trends observed in analytical and high fidelity simulation results. Conclusions are presented in Section V.

II. Analytical Results for One-State Model

An exact analytical solution to solve the optimal control problem for a first-order system with preview information was provided in [9]. This section applies a simplified version of the results in [9] for rotor speed tracking in above-rated wind conditions (Region 3). The control objective is to minimize the peak tracking error. The L_∞ (peak) norm is used to measure the tracking error for two reasons. First, minimizing the peak rotor speed error is crucial to avoiding generator over-speed. Second, variations in rotor speed are correlated to structural loads on the turbine. Hence reducing variations in rotor speed typically leads to reduced peak blade, tower and gearbox loads. Peak loads encountered under extreme wind conditions are a driving design factor for large, commercial wind turbines that contain highly flexible structures.

The wind turbine considered for the analysis is the three-bladed Controls Advanced Research Turbine (CART3) located at the National Wind Technology Center (NWTC). The CART3, shown in Figure 1, is a $40\ m$ diameter turbine with $600\ kW$ rated power. The CART3 is chosen for this study because it has been used extensively in the literature. This provides the opportunity to understand performance trends observed in previous work on preview control for wind turbines [4] and [5] in the context of the analytical results provided in this paper.

A. Modeling

A one-state linear turbine model is obtained as follows. The power captured by the turbine is given by [1]:

$$P = \frac{1}{2}\rho\pi R^2 v^3 C_p(\lambda,\beta) \tag{1}$$

where ρ is the air density (kg/m^3), R is the rotor radius (m) and v is the average wind speed over rotor area (m/s).

Fig. 1. The Controls Advanced Research Turbine (CART3) at the NWTC site at Golden, CO. Photo courtesy of Benjamin Sanderse from Energy Research Centre of the Netherlands.

$C_p(\lambda,\beta)$ is the nondimensional power coefficient as a function of the blade pitch angle β (deg) and the tip speed ratio $\lambda := \frac{R\omega}{v}$ where ω is the rotor speed (rad/s). The aerodynamic torque τ_a ($N\cdot m$) is given by:

$$\tau_a = \frac{P}{\omega} \tag{2}$$

A simple model of the rigid-body rotor dynamics can be obtained using Newton's law:

$$\dot{\omega} = \frac{1}{J}(\tau_a - \tau_g) = \frac{1}{J}\left(\frac{\rho\pi R^2 v^3 C_p(\lambda,\beta)}{2\omega} - \tau_g\right) \tag{3}$$

where J is the rotor inertia ($kg\cdot m^2$) and τ_g is the generator torque ($N\cdot m$). The $C_p(\lambda,\beta)$ data is usually available in lookup tables. Eq. (3) has one state (ω), two control inputs (τ_g and β) and one exogenous disturbance (v). Equation (3) can be numerically linearized at a trim condition $(\bar{\omega},\bar{\tau}_g,\bar{\beta},\bar{v})$ to obtain a one-state model of the form:

$$\delta\dot{\omega}(t) = a\ \delta\omega(t) + b\ \delta\beta(t) + c\ \delta v(t) \tag{4}$$

The δ symbol in front of the variables denote deviations from trim values $\bar{\omega}$, $\bar{\beta}$ and $\bar{v}$. The constant coefficients a, b and c in this linear model correspond to the damping, control gain, and disturbance gain, respectively. We are considering Region 3 control. In this region, the generator torque (τ_g) is typically held fixed for constant power and blade pitch (β) is used for control. Thus the input $\delta\tau_g$ is neglected in Equation (4). In addition, the Region 3 trim condition $\bar{\omega}$ is the rated rotor speed and hence $\delta\omega(t)$ is the rotor speed tracking error. The control

objective is to regulate $\delta\omega(t)$ to zero. The disturbance is "matched" in Equation 1 and hence it can be perfectly canceled by setting $\delta\beta(t) = -\frac{c\delta v(t)}{b}$. However, perfect cancellation is not possible if the actuator is subject to rate constraints and the wind speed is rapidly changing. An advanced sensor, e.g. LIDAR, can be used to generate a preview measurement of the wind disturbance, i.e. a measurement of $\delta v(\tau)$ for $\tau > t$. This preview measurement can be used to partially overcome the disturbance rejection limitations imposed by actuator rate constraints.

B. Problem Formulation

Assume the controller has access to T seconds of preview wind information. The essence of the performance vs. preview trade-off is captured by the following control optimization problem:

$$\begin{aligned} p(T) := \min_{\dot\beta \in C[-T,\infty)} \quad & ||\delta\omega||_\infty \\ \text{subject to: Equation (4)} \quad & \\ & |\dot\beta(t)| \le r \\ & \delta\omega(-T) = 0, \delta\beta(-T) = 0 \\ & \delta v_T(t) = \begin{cases} 0 & \text{if } t < 0 \\ v^* & \text{if } t \ge 0 \end{cases} \end{aligned} \tag{5}$$

where $C[-T,\infty)$ is the vector space of continuous functions defined on the interval $[-T,\infty)$. The infinity-norm for the continuous signal $\delta\omega$ is defined as $||\delta\omega||_\infty = \sup_{t\in[-T,\infty)} |\delta\omega(t)|$. In words, the turbine is initialized at the equilibrium $\delta\omega(-T) = 0$ and is disturbed by a wind gust of magnitude v^* at time $t = 0$. The objective is to design the optimal pitch input that minimizes the peak deviation in $\delta\omega$. Here the pitch rate constraint is written as $|\dot\beta| < r$ without the symbol δ since the trim pitch rate $\bar{\dot\beta}$ is zero. $\delta\beta$ is rate constrained and hence the wind gust cannot be perfectly canceled. The control problem formulation allows $\delta\beta$ to anticipate the disturbance, i.e. the blades can begin moving at $t = -T$ to cancel the step gust at $t = 0$. This models a situation in which the controller has a measurement of the disturbance with T seconds of preview. $p(T)$ denotes the optimal performance as a function of the preview time T. The rest of the presentation assumes, without loss of generality, that $v^* \ge 0$.

The step wind gusts used in this formulation do not fully capture the effects of turbulent wind conditions. However, the frequency spectra of many common turbulence models [11] exhibit a roll-off characteristic similar to of a step gust. Hence step wind gusts can provide a useful approximation to the turbine performance under turbulence.

The frequency spectrum of the turbulent wind conditions generated for CART3 is shown in Figure 2 (solid line). TurbSim [11], developed at NWTC, was used to generate the turbulent wind data. The parameters for generating the turbulent wind data are taken from the work by Laks, et al. [5] and are listed in the Table I. These wind conditions are considered to be realistic for the NWTC site where the CART3 is located. The average wind speed of 18 m/s was chosen to ensure constant Region 3 operation. The wind conditions

Parameter	Value
Mean Wind Speed	18 m/s
Vertical Wind Shear (α_0)	0.110
Vertical Stability (Ri_{TL})	-0.18
Mean Friction Velocity (U_{*D})	0.682 m/s

TABLE I
ATMOSPHERIC PARAMETERS USED IN TURBSIM FOR GENERATING TURBULENT WIND DATA

generated by TurbSim include spatial and temporal variations. Only the frequency spectrum of the hub-height average wind minus the trim wind speed is shown. The dash-dotted line in Figure 2 is the spectrum of a 2.5 m/s step wind gust. The spectrum of the step gust is a good approximation for the turbulent spectrum over a wide frequency band of 0.01 to 25 rad/s. The dashed curve in Figure 2 is the H_∞ design weight used to describe the expected spectrum of the disturbances. This curve and weight will be discussed further in the next section.

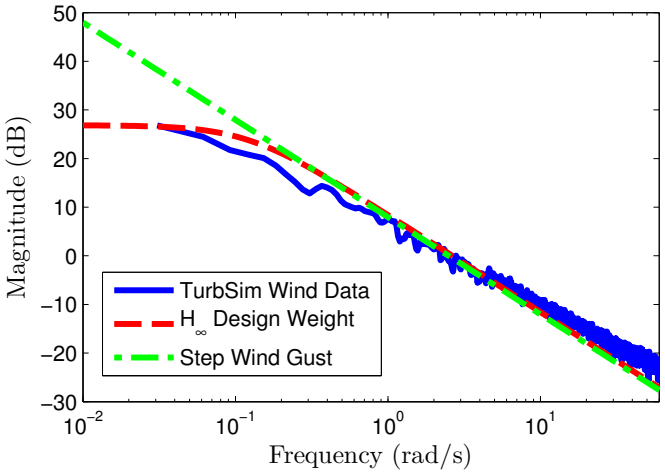

Fig. 2. Frequency spectrum of the hub-height average speed of the turbulent wind conditions

The CART3 model [12] is trimmed at $\bar v = 18$ m/s for Region 3 linearization. This is approximately the mean of the rated and cut-out wind speed specifications for this turbine. The rated rotor speed, generator torque and corresponding trim pitch angles are $\bar\omega = 3.881$ rad/s, $\bar\tau_g = 152130$ $N\cdot m$, and $\bar\beta = 16.52$ deg. The resulting numerical values of a, b and c are -0.2771 $(rad)^{-1}$, -0.0527 $(deg\cdot s^2)^{-1}$ and 0.0731 $(m\cdot s)^{-1}$. A step wind gust of $v^* = 2.5$ m/s on top of the 18 m/s steady wind was used for the problem formulation in Equation (5). This amplitude was obtained from fitting the turbulent wind spectrum used for CART3 simulations with of a step gust as shown in Figure 2. The only remaining parameter in the optimal control problem (Equation (5)) is the pitch rate limit r. The CART3 pitch actuators have rate limits of 18 deg/s. The design value of the actuator rate limit is chosen as $r = 6$ deg/s for this analysis. This is because a controller designed to yield 6 deg/s peak pitch rate for step wind gusts is expected to use higher pitch rates in turbulent

wind.

The remainder of this section provides the optimal pitch control as a function of the preview time. Additional details, including proofs of optimality, can be found in [9]. The optimal solution consists of four cases: zero, small, medium, and large preview times. The characterizations of these four cases depends on a fundamental preview time defined as $T^* := \frac{cv^*}{r|b|}$. In addition, the optimal solution depends on the non-dimensional decay rate $\alpha := aT^*$. For the CART3 linearization data the constants are $T^* = 0.577\ s$ and $\alpha = -0.160$. The results are presented for the approximation that $\alpha = 0$ (equivalently $a = 0$). This introduces less than 1% error because $\alpha \ll 1$ for the CART3 data. More importantly, this approximation leads to simpler analytical formulas that can be used to gain insight into the preview control problem. This approximation arises because a utility-scale wind turbine has a large rotor inertia. The large inertia translates into a small decay rate a relative to the fundamental time scale T^* that arises in the preview control problem, i.e. $aT^* \ll 1$. The exact amount of error introduced by this approximation can be obtained by comparing the full solution presented in [9] to the simplified results presented here.

C. No Preview: $T = 0$

If there is no preview ($T = 0$) then the optimal response is to ramp the blades at their maximum rate $\dot{\beta} = r$ until $\delta\beta$ cancels the wind gust. It takes $T^* := \frac{cv^*}{r|b|}$ seconds to pitch the blades $\delta\beta$ from 0 to $\frac{cv^*}{|b|}$. This optimal input can be written as:

$$\delta\beta_0(t) = \begin{cases} r(t+T) & \text{if } -T \le t < T^* - T \\ \frac{cv^*}{|b|} & \text{if } t \ge T^* - T \end{cases} \tag{6}$$

Integration of the system dynamics (Equation (4)) with $a = 0$ yields the trajectory:

$$\delta\omega_0(t) = \begin{cases} cv^*(t+T) - \frac{|b|r(t+T)^2}{2} & \text{if } -T \le t < T^* - T \\ \frac{(cv^*)^2}{2r|b|} & \text{if } t \ge T^* - T \end{cases} \tag{7}$$

Therefore the minimal peak rotor speed tracking error (Equation 5) with no preview is given by $p(0) = \frac{(cv^*)^2}{2r|b|}$.

D. Small Preview: $T \le \left(\sqrt{2}-1\right)T^*$

For "small" preview times, the optimal pitch action is still given by $\delta\beta_0(t)$ in Equation 6. Specifically, $\delta\beta_0(t)$ is optimal for preview times that satisfy $T \le \left(\sqrt{2}-1\right)T^*$. Figure 3 shows the response of the turbine rotor with the optimal input $\delta\beta_0(t)$ for three different "small" preview times. The wind gust occurs at $t = 0$ for each response. The controller starts acting when the wind gust information enters the system at $t = -T$. In other words, the controller has exactly T seconds to act before the gust. The solid line in this figure is the response $\delta\omega_0(t)$ for no preview (Equation 7). For the CART3 data, $T^* = 0.577\ s$ and the minimal rotor speed error with no preview is $p(0) = 0.0527\ rad/s$. The dashed and dash-dotted lines are the optimal responses for $T = 0.1\ s$ and $T = 0.23\ s$. All three trajectories achieve their peak magnitude at $t = T^* - T$ and have $\delta\dot{\omega}(t) = 0$ for $t \ge T^* - T$.

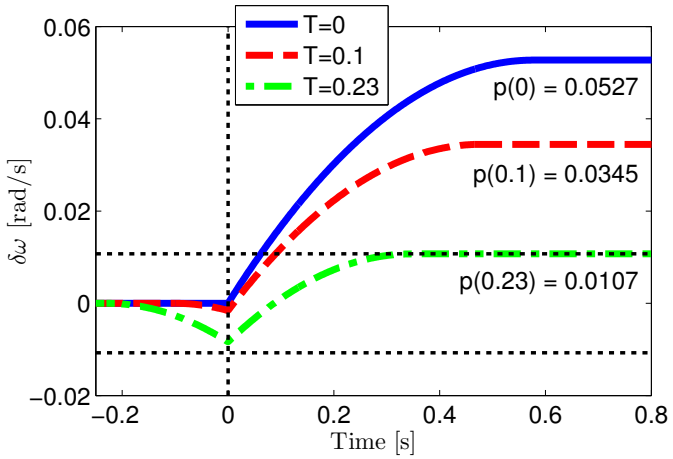

Fig. 3. Time responses of rotor speed error ($\delta\omega(t)$) for "small" preview times. The wind gust occurs at $t = 0$ for all responses

For $T = 0.1\ s$, the rotor speed is $\frac{-|b|r(t+T)^2}{2}$ at the onset of the step gust ($t = 0$). At $t = 0$, the rotor speed reverses direction due to the step wind gust and eventually reaches a steady state at $\delta\omega(T^* - T) = 0.0345\ rad/s$. The preview has two benefits. First, the control input is able to partially overcome the rate limit by pitching the blades toward $\frac{cv^*}{|b|}$ before the step wind gust occurs. Second, the initial negative motion of the rotor speed leaves the turbine in a better position to absorb the wind disturbance. In particular, the large positive peak at $\delta\omega(T^* - T)$ is reduced because disturbance must first overcome the negative value of $\delta\omega(0)$ at the time of the step gust. As a result the optimal cost is reduced from $p(0) = 0.0527\ rad/s$ to $p(0.1) = 0.0345\ rad/s$.

The response for $T = 0.23\ s$ shows a similar trend with the error further reduced to $p(0.23) = 0.0107\ rad/s$. Note that, for $T = 0.23\ s$, the negative motion of the rotor speed prior to the gust reaches $\delta\omega(0) = -0.0084\ rad/s$. This is very close to the magnitude at $\delta\omega(T^* - T) = 0.0107\ rad/s$. As the preview time is further increased, the error at the time of the gust, $\delta\omega(0)$, continues to become more negative (larger in magnitude). In addition, $\delta\omega(T^* - T)$ continues to decrease in magnitude. This trend continues until T becomes large enough that $|\delta\omega(0)| = |\delta\omega(T^* - T)|$. The two peaks are precisely equal at $T = (\sqrt{2}-1)T^*$. For $T > (\sqrt{2}-1)T^*$, $\delta\beta_0$ in Equation (6) is no longer optimal because the blade pitch before the wind gust creates a negative peak at $\delta\omega(0)$ that dominates the cost. In other words, the control action before the gust specified in Equation (6) does more harm than good.

E. Moderate Preview: $\left(\sqrt{2}-1\right)T^* < T \le T^*$

For "moderate" preview times $(\sqrt{2}-1)T^* < T \le T^*$, the optimal pitch action is of the form:

$$\delta\beta_T(t) = \begin{cases} -r(t+T) & \text{if } -T \le t < t_1 - T \\ +r(t+T-2t_1) & \text{if } t_1 - T \le t < 2t_1 + T^* - T \\ \frac{cv^*}{|b|} & \text{if } t \ge 2t_1 + T^* - T \end{cases} \tag{8}$$

where $t_1 := \frac{T^2+2TT^*-T^{*2}}{4(T+T^*)}$. The subscript in $\delta\beta_T$ denotes that the optimal pitch action depends on T through the parameter t_1. For $t \leq t_1 - T$ the optimal input $\delta\beta_T$ ramps the blades at maximum rate in the wrong direction, i.e. away from the value $\frac{cv^*}{|b|}$ required to cancel the step wind gust. Then it ramps the blades at maximum rate in the other direction until it reaches $\frac{cv^*}{|b|}$. As noted above, the optimal cost for preview time $T = (\sqrt{2}-1)T^*$ becomes constrained by the negative peak at $\delta\omega(0)$. The magnitude of $\delta\omega(0)$ is reduced by ramping the blades initially in the wrong direction. The initial pitching in the wrong direction allows the system to be closer to the final pitch angle at the time of gust ($t = 0$) without causing a larger rotor speed error.

Figure 4 shows the rotor speed response and optimal input $\delta\beta_T(t)$ for three different "moderate" preview times. The solid, dashed, and dash-dotted lines are the responses for $T = 0.3$ s, 0.4 s, and $T^* = 0.577$ s. All three trajectories have $\delta\dot{\omega}(t) = 0$ for $t \geq 2t_1 + T^* - T$. For each preview time the state trajectory $\delta\omega(t)$ achieves the peak magnitude $p(T)$ at both $t = 0$ and $t = 2t_1 + T^* - T$. In other words, the value of t_1 is chosen to balance both the negative peak at $\delta\omega(0)$ and the positive peak at $\delta\omega(2t_1 + T^* - T)$.

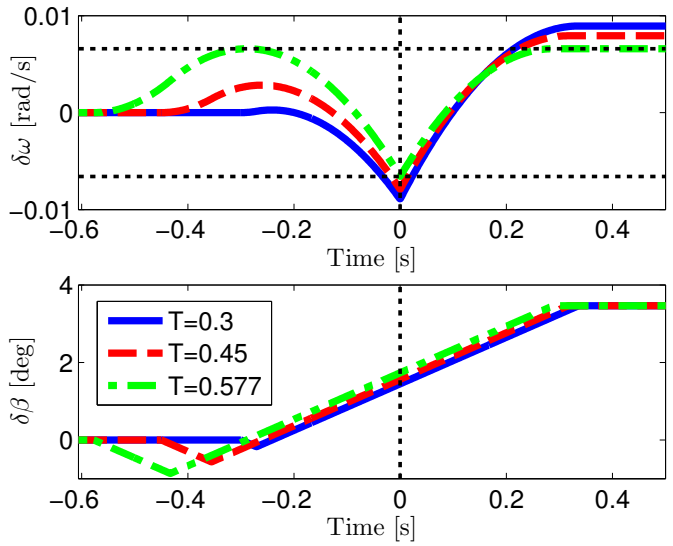

Fig. 4. Time responses of rotor speed error ($\delta\omega(t)$) and optimal pitch command ($\delta\beta(t)$) for "moderate" preview times. The wind gust occurs at $t = 0$ for all responses

For each trajectory the optimal control $\delta\beta_T$ is negative for $t < 2t_1 - T$. This causes $\delta\omega(t)$ to initially move in the positive direction and achieve a local maximum at $\delta\omega(2t_1 - T)$. As the preview time T increases, $\delta\omega(2t_1 - T)$ becomes more positive while the magnitudes of $\delta\omega(0)$ and $\delta\omega(2t_1 + T^* - T)$ are both reduced. When $T = T^*$ the first positive peak at $t = 2t_1 - T$ satisfies $|\delta\omega(2t_1 - T)| = |\delta\omega(0)| = |\delta\omega(2t_1 + T^* - T)|$. For $T > T^*$, the input $\delta\beta_T$ in Equation 8 is no longer optimal because the magnitude of $\delta\omega(2t_1 - T)$ dominates the cost. For the given data, $T^* = 0.577$ s and hence the dash-dotted curve in Figure 4 represents the optimal response for the limiting case of "moderate" preview ($T = T^*$). The optimal input $\delta\beta$ shown in the bottom subplot changes from $\delta\dot{\beta} = -r$ to $\delta\dot{\beta} = +r$ at $t_1 - T$. The top subplot shows that the optimal $\delta\omega(t)$ for $T = 0.577$ s achieves its maximum magnitude at times $2t_1 - T$, 0, and $2t_1 + T^* - T$.

One issue may arise with "moderate" preview times when the wind speeds are just above the rated wind speed required for Region 3 operation. The initial blade pitch action with $\delta\dot{\beta} = -r$ is limited in this situation since the blades may hit the β lower-bound of pitch-to-feather turbines. This means the blade pitch angles cannot be lowered any more to gain rotor speed before the gust. In this case the performance can be conservatively considered to be bounded by the performance given with "small" preview times. This is a limited performance loss since "moderate" preview times yield limited performance improvement as seen in Figure 5.

F. Long Preview: $T > T^*$

For $T > T^*$ one might suspect that $p(T)$ can be further reduced by pre-pending the control action $\delta\beta_{T^*}(t)$ with an initial negative ramp of the blades. This might simultaneously reduce the magnitudes of $\delta\omega(2t_1 - T)$, $\delta\omega(0)$, and $\delta\omega(2t_1 + T^* - T)$ which constrain the performance for $T = T^*$. In actuality, no further improvement can be obtained for $T > T^*$, i.e. there is a fundamental bound on the performance improvements achieved via preview. This fact is formalized in the following theorem:

Theorem. *$p(T) = p(T^*)$ for all $T \geq T^* = \frac{cv^*}{r|b|}$. The minimal cost is $p(T^*) = \frac{(cv^*)^2}{16r|b|}$*

Proof: *Follows from reference [9].*

The optimal input for $T > T^*$ is not unique but one choice is given by:

$$\delta\beta_T(t) = \begin{cases} 0 & \text{if } t < -T^* \\ \delta\beta_{T^*}(t) & \text{if } t \geq -T^* \end{cases} \tag{9}$$

where $\delta\beta_{T^*}$ is the optimal input given by Equation (8) for $T = T^*$. This choice wastes the first $T - T^*$ seconds of preview by leaving the input at zero and then executes the control action $\delta\beta_{T^*}$ once T^* seconds of preview remains.

G. Summary

The solution to the optimal control problem (Equation (5)) for $a = 0$ (no damping in Eq. (4)) is summarized in Table II. Figure 5 shows the minimal peak rotor speed error versus preview time. $T^* = \frac{cv^*}{r|b|}$ is a fundamental preview time beyond which no additional performance improvements are obtained. The fundamental preview time and optimal tracking cost $p(T^*)$ are both inversely related to the rate limit r and control gain b in Eq. (4). T^* grows linearly with increasing magnitude of the wind gust v^* and disturbance gain c while $p(T^*)$ grows quadratically. In addition, $p(0) = \frac{(cv^*)^2}{2r|b|}$ and $p(T^*) = \frac{(cv^*)^2}{16r|b|}$. Thus, preview information can, at best, reduce the peak tracking error by a factor of eight compared to the performance with no preview. Finally, the use of preview has the largest impact for $T \leq (\sqrt{2}-1)T^*$. For these small preview times, the rotor speed error reduces linearly in T. Only minor improvements in the cost are obtained for preview times $(\sqrt{2}-1)T^* < T \leq T^*$.

Preview Time	Optimal Cost, $p(T)$	Optimal Input, $\delta\beta(t)$
$T \leq (\sqrt{2}-1)T^*$	$\frac{(cv^*)^2}{2r\lvert b\rvert} - cv^*T$	Equation 6
$(\sqrt{2}-1)T^* < T \leq T^*$	$\frac{\lvert b\rvert r}{16}\frac{(-T^2+2TT^*+T^{*2})^2}{(T+T^*)^2}$	Equation 8
$T > T^*$	$\frac{(cv^*)^2}{16r\lvert b\rvert}$	Equation 9

TABLE II
SUMMARY OF RESULTS FOR $a = 0$

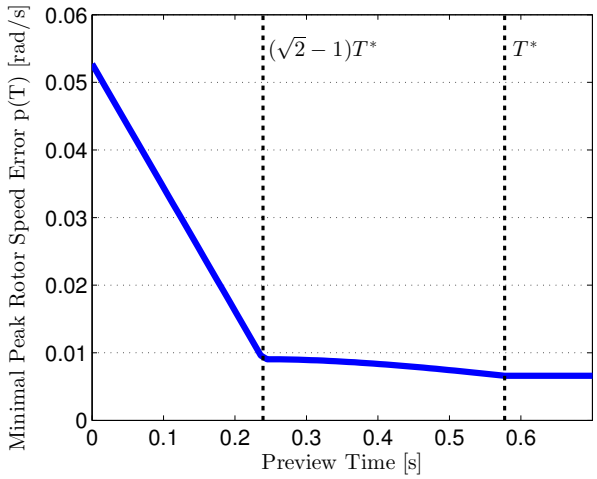

Fig. 5. Performance versus preview time predictions from analytical results

H. Effect of Operating Condition

The results presented in the previous sub-sections are based on a 1-state rigid body model of the CART3 trimmed at 18 m/s. The parameters a, b and c of this model change with the mean wind speed. We have obtained linearizations from the rated wind speed of the CART3, 12.5 m/s, up to 24 m/s to investigate the effect of operating conditions on preview time requirements. The b and c parameters from each of these models are used to calculate the fundamental preview time $T^* = \frac{cv^*}{r|b|}$. Figure 6 shows the T^* versus the trim wind speed. The $T^* = 83$ s calculated for 12.5 m/s trim wind condition is not plotted. This is because T^* decreases rapidly with increasing trim wind speed. Trim pitch angle difference between 12.5 m/s and 12.6 m/s is approximately 1.5 deg. Blades with the pitch rate limit 18 deg/s can travel 1.5 deg in a much shorter time than the difference in the fundamental preview times between these two trim wind speeds.

The preview time versus trim wind speed trend observed in Figure 6 agrees well with general turbine design considerations. This trend is largely driven by the variations in the control gain parameter b. Turbine power and torque capture are designed to be insensitive to pitch angle variations around the optimal pitch angle for power capture in Region 2. This corresponds to a small b value. This is in order to minimize power losses due to uncertainties related to calculation of this optimal pitch angle. As the turbine enters Region 3, the pitch angle is increased to shed some of the power in wind. To achieve this effect the turbine design favors a higher b value at increasing pitch angles. For instance, $b = -0.0070$ and -0.0260 at trim wind speeds equal to 12.6 m/s and 14 m/s, respectively. The fundamental preview time T^* is inversely related to b. Hence the increase in control effectiveness b from 12.6 m/s to 14 m/s corresponds to the decrease in fundamental preview time.

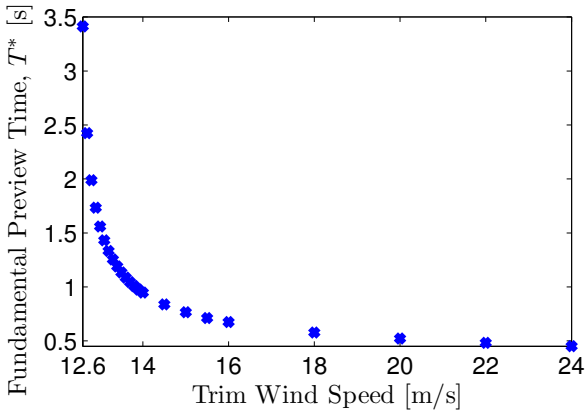

Fig. 6. Fundamental preview time versus trim wind speed

III. H_∞ PREVIEW CONTROL FOR CART3 TURBINE

This section presents an H_∞ preview controller using a design architecture similar to that used by Laks, et al. [4]. This is a 2-input (rotor speed and wind speed measurements) and 1-output (collective pitch) controller. The performance vs. preview time is evaluated using the NWTC's Fatigue, Aerodynamics, Structures, and Turbulence (FAST) nonlinear simulation code [13]. A detailed LIDAR sensor model is implemented to capture the challenges associated preview wind sensing. The performance trends for this higher fidelity model are compared with the trends predicted by the simple, rigid-body analysis described in the previous section.

FAST can model onshore wind turbines with a total of 22-24 degrees of freedom. The nonlinear FAST model contains the effects of aeroelasticity and structural dynamics which are not captured by the one-state model. FAST has been validated against ADAMS and Germanischer Lloyd turbine simulation codes [14]. It has been certified by Germanischer Lloyd that it is acceptable for turbine manufacturers to use FAST for onshore turbine certification. The high-fidelity FAST model of CART3 used for simulations included first and second tower fore-aft and side-to-side bending modes, first and second flapwise bending modes of blades, first edgewise bending modes of blades, drivetrain torsion, generator position. The basic FAST code does not include models for pitch actuator dynamics and rate limits. The dynamics of the CART3 pitch actuators are represented by first-order models with time constants of $\tau = 1/30$ s [4]. In addition, the CART3 pitch actuators have a rate limit of 18 ^{o}/s. All FAST simulations included these first order pitch actuator models with rate limits.

A detailed model of the ZephIR LIDAR [15], a commercially available continuous wave LIDAR, is implemented with

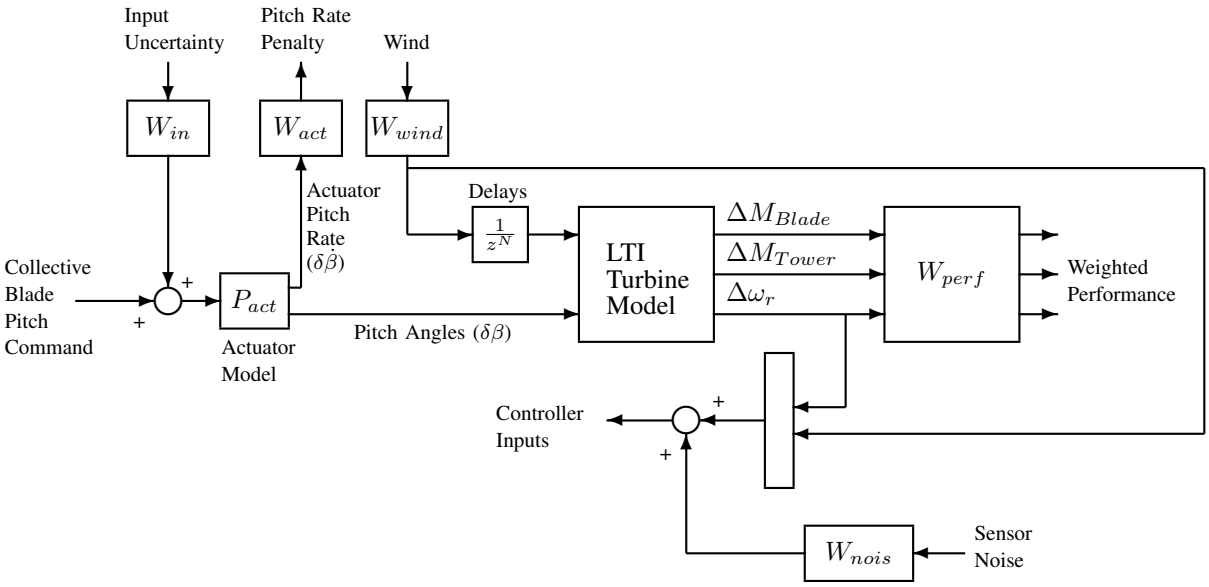

Fig. 7. System Interconnection for H_∞ Collective Pitch Controller Design

FAST for high-fidelity simulations. This model is based on the work in Reference [16]. It is assumed that the LIDAR is mounted at the turbine hub in a forward looking fashion and spinning with the rotor. The LIDAR itself also contains an internal spinning mechanism that allows its laser beam to be directed in any direction during operation independent of the rotor angle. It is assumed that the LIDAR is supplying the average of the wind measurements at three points in space to the controller. In other words, the spinning mechanism in the LIDAR is used to direct the laser beam in three directions during one sample time of the controller. The location of these three points depend on the preview time and the desired measurement point on the blade span. 75% blade span or $15\ m$ from the rotor hub is chosen since most of the power capture is obtained at the outer section of the blades. The future position of the blades is estimated by a constant rotor speed assumption during the preview time.

This LIDAR model is implemented with the FAST Simulink model by reading the full-field turbulent wind files generated by TurbSim before the simulation. bf These files describe the wind speed across the rotor plane at zero yaw angle as a function of time. This wind information is unfolded in space with the assumption of Taylor's frozen turbulence hypothesis [17]. It is assumed that the wind is traveling at a constant speed which is the mean horizontal wind speed at the hub-height throughout the wind file. FAST time-shifts the data in the full-field wind files before the simulation starts. This is in order to contain the turbine rotor in the wind field for any initial yaw angle. The exact time-shift in seconds is 0.5 times the ratio of the total width of the wind data grid (m) and the mean horizontal wind speed at hub-height (m/s) [11]. This width is defined as the size of the grid in the perpendicular direction to the vertical in the rotor plane.

The LIDAR sensor measures a weighted average of the wind speed along its beam in three dimensional space. The use of this model incorporates two error sources for wind measurements. The first source of error stems from the fact that LIDAR cannot measure wind measurements at a fixed point in space. The measurements from continuous wave LIDARs involve a spatial weighting across the laser beam. This weighting is given by a Lorentzian function. This function depends on the focus distance. Longer focus distances correspond to more averaging. This introduces higher errors with increasing focus distance or preview time. The second type of error arises from the orientation of the laser beam. The wind speed measurement of interest is the wind in the horizontal direction at the desired blade span. A large angle between the horizon and the laser beam means that the projection of the horizontal wind on the laser beam will be limited. Instead, the vertical and side-wise wind speeds will corrupt the measurement. The error increases with smaller preview times and measurements that are farther away in the transverse (perpendicular to earth surface) direction from the rotor hub.

There are two more error sources that need to be considered. The first source of error arises from the fact that it is not possible to know the future rotor position. A simple predictor that assumes a constant rotor speed for the duration of preview is used to predict the future position of the blades. This prediction error increases with increasing preview times. The second error source is the assumption of the Taylor's frozen turbulence hypothesis, but this effect is not captured in our high-fidelity simulations. In other words, the evolution of the wind field from the measurement point to the turbine is ignored. The impact of this assumption depends on the preview time. This effect can be studied with use of an advanced computational fluid dynamics code. However, this is beyond the scope of this study. Note that the two error sources described in this paragraph are not directly tied to the LIDAR sensor model.

A low order model of the CART3 was used for the control

design. The low order, 5 degrees of freedom design model contained modes for generator speed, tower first fore-aft bending and blade first flapwise bending. This model is based on a linearization of the FAST model of the CART3 at the trim conditions specified in the Section II-B. The turbine dynamics depend on rotor position and have a non-steady trim trajectory. Hence linearizations are performed on a grid of rotor positions and result in linear time-varying (LTV) models. This LTV model is converted to an LTI model using the multi-blade coordinate transformation [18]–[22] followed by averaging of the resulting matrices. Finally, the turbine model was discretized using a bilinear (Tustin) transformation with a sample time of $T_s = 0.025s$. This is the sample time used by the FAST model of the CART3. The discretization step was needed for modeling of the wind preview information. Finally, the first-order pitch actuator models with 30 rad/sec bandwidth were added to the design model. The final design model had 11 states.

A H_∞ preview controller is designed based on this reduced-order, discrete-time LTI model of the CART3. The control objective is rotor speed tracking as well as tower and blade load reduction at higher (Region 3) wind speeds. The control input is the collective pitch angle of three blades. The measurement for control is the rotor speed. In addition, it is assumed that the controller has access to preview measurements of the average wind speed across the rotor disk. The preview measurements are modeled by augmenting the wind disturbance input of the design model with N delays. The controller has access to a measurement of the wind disturbance input to the chain of N delays. As a result, the controller has a measurement of the wind disturbance with a preview of NT_s seconds prior to its impact on the turbine. The amount of preview available to the H_∞ controller is adjusted by changing the number of delays N.

Signal-weighted H_∞ control designs were performed for a variety of preview times N using the system interconnection shown in Figure 7. The block labeled "LTI Turbine Model" is the discrete-time LTI design model without the actuator dynamics and the N steps of delay on the wind input. The block P_{act} contains the pitch actuator model for CART3. The first output of this model is the actuator pitch rate and the second output is the pitch angle. The extra pitch rate output was created to penalize blade pitch rates to normalize control usage across all the designs. The system interconnection contains weights for performance, input uncertainty, measurement noise, actuator usage, and wind disturbance. These weights are briefly described and, unless stated otherwise, controller designs for all values of preview time share the same weights. The weights were initially specified in continuous-time and then converted to discrete-time using a bilinear (Tustin) transformation with a sample time of $T_s = 0.025s$.

The continuous-time transfer functions for each weight are provided in the Appendix A. The performance weight is block diagonal $W_{perf} = diag(W_{BladeM}, W_{TowerM}, W_{\omega_r})$ with the individual blocks penalizing flapwise collective blade bending moment, tower fore-aft bending moment, and rotor speed tracking respectively. The performance penalty W_{BladeM} emphasizes attenuation of the blade bending moment at middle to high frequencies. This choice is made because the DC and lower frequency components of the blade bending moments, due to persistent wind disturbances, cannot be attenuated. The penalty weight on the tower bending W_{TowerM} is chosen to add extra damping at the tower bending moment frequency. The performance penalty W_{ω_r} is chosen to attenuate low-frequency tracking errors. The input disturbance W_{in} models dynamic uncertainty across all frequencies. The weight W_{nois} is a 2×2 diagonal weight that models noise on the rotor speed and wind speed, respectively. The rotor speed and wind speed measurement noise weights are chosen as a high pass to avoid excitation of the high-frequency modes of the turbine. A constant weight is used for the wind speed measurement noise to model measurement noise across all frequencies. The actuator weight W_{act} is used to penalize the blade pitch rates. This penalty acts directly on the pitch rates as opposed to the pitch command rates. The gain of the constant weight K is chosen as a function of the wind preview time N. The value of K is tuned through simulations to obtain a closed-loop peak pitch rate of 6 deg/s for a 2.5 m/s uniform wind gust input for all H_∞ controllers of different preview lengths. This ensures that controllers for all preview times have roughly the same actuator usage. This normalization is carried out so that the H_∞ controllers have the same peak pitch rate with the analytical solutions presented in the previous section. Values of gain K versus preview time are provided in Table IV in Appendix A.

One design weight of particular importance is the weight on the wind disturbance W_{wind}. This weight represents the frequency spectrum of the operating wind conditions. This spectrum is important because the preview time required for optimal pitch action depends on the turbulent wind conditions. For instance slow wind variations with small magnitude require smaller preview times. Larger magnitude fluctuations observed in higher turbulence require longer preview times. The weight W_{wind} used in this design is obtained from time-series turbulent wind data generated by TurbSim as described in the Section II-B. The frequency spectrum of this wind profile, shown in Figure 2, is fit with a first-order transfer function to obtain W_{wind}. The preview time required by the H_∞ controllers depend on this weight. This is similar to the fact that the fundamental preview time T^* is related to the step wind gust magnitude v^* used in the analytical results.

IV. Results

The effect of preview time on the closed-loop performance for the H_∞ preview controllers was evaluated on the nonlinear FAST model of the CART3 with the LIDAR sensor model. All degrees of freedom available in FAST for onshore turbines, except the yaw, rotor furl and tail furl DOF, were used in the simulations. The first order actuator dynamics and rate limits were included in the simulation model. The performance of the H_∞ preview controllers was evaluated with three sets of simulations. First, the closed-loop was simulated with the step wind gust that was used in the 1-state analysis. Second, simulations were performed under turbulent wind conditions but with ideal preview measurements at the $15m$ or 75%

span of each blade. The average of these measurements are fed to the collective pitch controller along with the rotor speed measurement. Note that this "ideal" measurement case is still impacted by the prediction errors regarding future rotor position. In the third set of simulations the controller uses an average of three measurements from the LIDAR model. These simulations use three dimensional full-field wind trajectories. This represents a more realistic sensing set up that captures the challenges associated with preview wind measurements. Specifically, wind measurement errors from spatial range weighting and projection of the horizontal wind onto the laser beam are incorporated on top of the errors caused by the rotor position prediction. Taylor's frozen turbulence assumption is used in the simulations, i.e. the evolution of the wind field from measurement to the impact on the turbine is neglected. This assumption impacts both the "ideal" measurement case and the LIDAR model.

A. Results with Ideal Measurements

The closed-loop response of the nonlinear CART3 system to a 2.5 m/s uniform wind step disturbance is shown in Figure 8 for H_∞ controllers with three different preview lengths. The solid, dashed, and dash-dot lines are the responses for the controllers with 0.0 s, 0.4 s, and 0.8 s of preview, respectively. The simulation results are time shifted such that the step wind gust occurs at $t = 0$. The controller with small 0.4 s preview starts pitching the blades as soon as information about the incoming gust in received ($t = -0.4s$). The control action looks similar to that of the no-preview controller but time-shifted by 0.4 s. This behavior shows close agreement with the predictions from the analytical results, i.e. similar pitch action for small and no preview. As the preview time increases further 0.8 s, the controller starts pitching the blades earlier at $t = -0.8$ s. The additional preview enables the controller to achieve larger pitch angles at the time of the gust ($t = 0$) than the other controllers. The H_∞ controller achieves a much smaller error by having a more negative (larger in magnitude) error before the gust. The H_∞ controllers with preview times larger than 0.8 s yield very similar results to the controller with 0.8 s preview and are not plotted. The long preview time (0.8 s) used here is slightly longer than the $T^* = 0.577$ calculated with the analytical results. The initial pitching toward the fine pitch angle with long preview times observed with analytical results are not seen here. The analytical result uses the L_∞ (peak) norm to measure performance while the H_∞ norm is induced by the L_2 (power) norm on signals. We believe the difference in behavior is simply due to this difference in the objective functions of the optimizations.

Figure 9 summarizes the rotor speed tracking performance of the H_∞ controllers on the nonlinear FAST simulations with step and turbulent wind gusts with ideal three point measurements of the wind field. The stars represent H_∞ controllers with step wind gusts. The circles are the H_∞ controllers in turbulent wind conditions. The triangles are the analytical solutions based on the one-state rigid body rotor model of the turbine. All nonlinear simulations with step gusts had peak pitch rates between 5.95 and 6.05 (deg/s). The

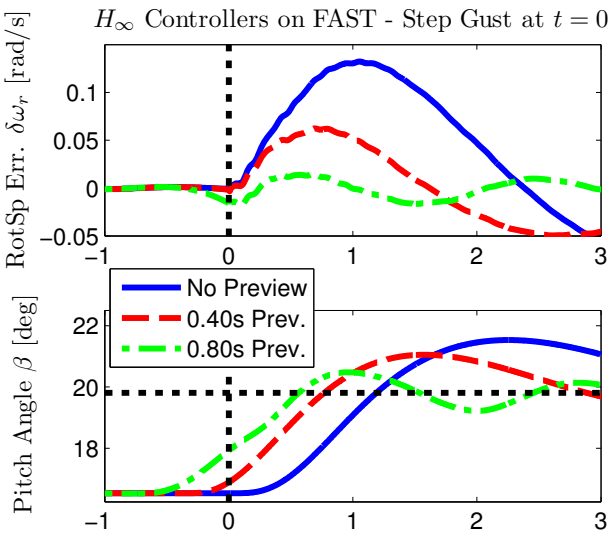

Fig. 8. Closed-loop response of the CART3 FAST model to a 2.5 m/s step uniform wind gust. The wind gust occurs at $t = 0$ for all responses

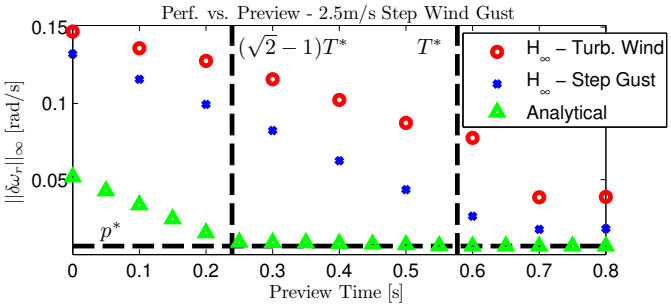

Fig. 9. Peak rotor speed error vs. preview time for step and turbulent wind for H_∞ controllers on FAST simulations. Ideal three point measurements of the wind field is used.

nonlinear simulations in turbulent wind had peak pitch rates between 4.75 and 7 (deg/s). The vertical lines in this plot correspond to the "small" and "long" preview times predicted by analytical solutions.

There are three key observations in Figure 9. First, the peak rotor speed error is reduced linearly with small preview times both for H_∞ controllers and analytical solutions. Second, there is a preview time beyond which no performance improvements are obtained. Third, the performance of the H_∞ controllers in the full nonlinear CART3 simulations with turbulent and step wind are very close in terms of rotor speed tracking. The slope of the improvement and the ultimate performance bounds are captured accurately by the analytical results. However, the optimal preview times observed with the H_∞ controllers are slightly longer than the T^*. Our design iterations have shown that the optimal preview time for the H_∞ controllers depend strongly on the weight that capture the wind measurement noise. Actuator penalty and input uncertainties also play a role on this optimal preview time. More conservative controllers tend to use longer preview times.

Figure 10 presents the normalized, average blade damage equivalent loads on the nonlinear simulations. The normalizing factors for the step gusts and the turbulent wind conditions

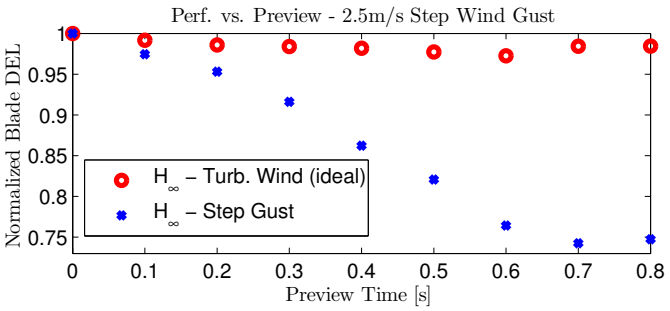

Fig. 10. Normalized, average blade DELs vs. preview time for step and turbulent wind for H_∞ controllers on FAST simulations. Ideal three point measurements of the wind field is used.

are 220 and 328 respectively. The reduction in blade damage equivalent loads is almost linear with small preview times with step wind gusts in step wind gusts. Similar to the rotor speed tracking performance, this improvement continues until $0.8\ s$ preview. The improvement between $0\ s$ preview and $0.8\ s$ preview are approximately 25%. This validates the correlation between rotor speed tracking and blade bending loads. However, these large improvements are not observed with the simulations under turbulent wind. The improvement obtained in this case is approximately 3%. Even though this performance depends on the design weights, we anticipate this gap to be due to the strong spatial variation of the wind over turbine blades with realistic full-field wind trajectories. This renders the use of collective pitch control for blade load reduction less effective. Individual pitch control with preview wind information may be used to address this issue.

The tower fore-aft bending moments and the RMS rotor tracking speed errors in step and turbulent wind conditions in FAST simulations are not shown here. These results follow the same trend as the peak rotor speed errors shown in Figure 9. Almost linear improvements are observed at low preview times and the improvements stop at $0.8\ s$ preview.

The results presented in this section are in agreement with the results in [4] which present the worst case gains of various H_∞ preview controllers designed for the CART3. The worst-case gain of the controller with $6\ deg/s$ pitch rate limit approximately flattens out at $0.65\ s$ of preview. This is a slightly shorter preview time than the one predicted here. But reference [4] does not use a frequency-based weighting for the wind disturbances. The optimal preview time depends on the design weight choice. Results in [4] also show that there is a fundamental performance limitation imposed by the pitch rate constraints regardless of the preview time. The worst-case gain versus preview time plots flatten out at a higher gain for controllers with smaller pitch rate bounds. This agrees with the results presented in Section II-F which shows that the optimal cost with long preview is inversely proportional to the pitch rate bounds.

B. Results with Realistic LIDAR Measurements

Figure 11 compares the performance of the H_∞ controllers with ideal measurements presented in Section IV-A to their performance with realistic preview wind measurements. These results capture the error characteristics of typical continuous wave LIDARs but use the Taylor's frozen turbulence hypothesis. The results with LIDAR models under $0.3\ s$ are not plotted since the large measurement errors from larger measurement angles from the horizon are extremely detrimental to turbine performance. The key conclusion from Figure 11 is that the error characteristics of the LIDAR sensors may require a longer preview time than the ones observed with the ideal measurements. The main reason behind this behavior is the large angle between the LIDAR beam and the horizon when trying to measure wind at the 75% blade span with small preview. The LIDAR measures the projection of the three dimensional wind speed along its beam. The increased angle between the horizon and the beam reduces the contribution of the horizontal wind speed to the measurement and increases the contributions of the transverse and side-wise wind speed. Increasing the preview time allows the LIDAR to obtain measurements at the same blade span with a smaller angle with the horizon. It is observed that the performance with realistic measurement get fairly close to the ideal performance with higher preview times. It should be noted that using too long preview times can also deteriorate the turbine performance. At long preview times the range weighting errors and the errors from the frozen turbulence hypothesis can dominate the measurement errors and be detrimental to turbine performance.

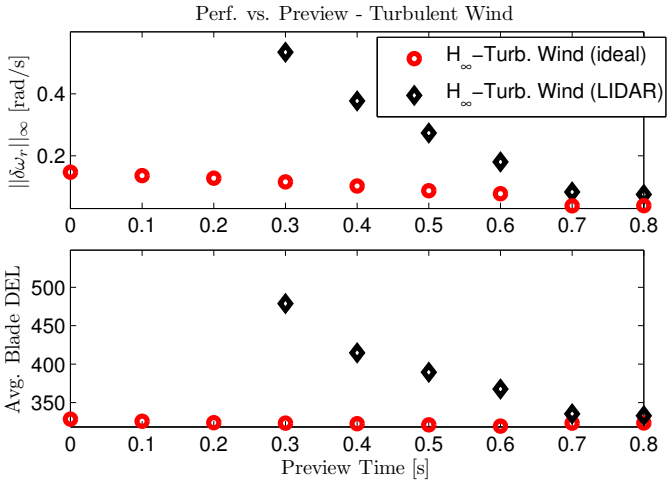

Fig. 11. Performance metrics vs. preview time for H_∞ controller simulations in turbulent wind and realistic LIDAR sensor models on FAST

C. Discussion

In summary, the performance of the advanced preview controllers depend on the pitch rate limits as well as the aggressiveness of the control design. The analytical formulas provide a method to predict the performance limits and trends for these controllers before any detailed control design. The simple steps taken for these predictions can be summarized as follows. A one-state nonlinear model that captures rigid-body rotor dynamics is linearized to obtain (a, b, c) parameters. The analytical results presented in Section II depend on a step wind gust magnitude. This gust magnitude is obtained

from the frequency spectrum of realistic turbulent wind conditions for turbine site. The second parameter required for the analytical solutions, the peak blade pitch rate, is obtained from simulation of the H_∞ controllers with step wind gusts. It is important to test the final controllers in high fidelity simulations with LIDAR sensor models. It was observed that the error characteristics of these sensors may necessitate use of longer preview times than the ones predicted by the analytical formulas.

V. Conclusion

This paper investigated performance limits for Region 3 turbine control using preview wind measurements. Three three key conclusions can be drawn from these results. First, performance improves linear with small preview times. Second, there is a fundamental preview time beyond which no additional performance improvement can be obtained. Third, this fundamental preview time is proportional to the step gust magnitude and inversely related to pitch actuator rate limit. The conclusions were validated with more realistic CART3 nonlinear simulations. The higher fidelity simulations showed similar trends for rotor speed tracking and tower structural loads. However, it was also observed that the error characteristics of the preview wind sensors can play an important role in turbine performance. Thus longer preview times may be required than those predicted from the low fidelity model.

Appendix A
H_∞ Controller Design Weights

Table III lists the design weights used in the H_∞ controller design interconnection shown in Figure 7. The design weights specified in continuous-time are discretized at the sample time of $T_s = 0.025\ s$ via bilinear (Tustin) transformation for the discrete H_∞ controller design. All weights except W_{act}, which penalizes the pitch command rate, are independent of the preview time. Table IV lists the constant gains used for pitch command penalty W_{act} as a function of the preview time. The second column of this table, denoted as "Delay States (N)", lists the number of delay states used in the design interconnection to model preview wind information.

The continuous-time LTI turbine model obtained by linearization, multiblade coordinate transformation [21] followed by averaging has the form of:

$$\begin{aligned}\dot{x} =& Ax + Bu\\ y =& Cx + Du\end{aligned}$$

This system is similarly discretized at $T_s = 0.025\ s$ via bilinear (Tustin) transformation for the discrete H_∞ controller design. The first two states of this linear system are the tower 1^{st} tower fore-aft bending mode tip-displacement (m) and rotor position (rad). The next three states correspond to the collective and cyclic 1^{st} blade flapwise bending mode displacements. States 6-10 are the derivatives of the first five states. The system inputs are the hub-height wind disturbance (m/s) and collective blade pitch angles (rad). The outputs are the collective blade flapwise root bending moment $(kN \cdot m)$, tower base fore-aft bending moment $(kN \cdot m)$ and rotor speed (rpm).

Weight	Transfer Function
W_{ω_r}	$0.002\frac{s+50}{s+0.05}$
W_{BladeM}	$2\times10^{-7}\frac{s+50}{s+0.2}$
W_{TowerM}	$5\times10^{-7}\frac{s+50}{s+5}$
W_{in}	0.03
W_{n,ω_r}	$1.5\frac{s+0.1}{s+5}$
$W_{n,wind}$	$15\frac{s+0.5}{s+75}$
W_{wind}	$\frac{2.64}{s+0.12}$
W_{act}	$K(N)$

TABLE III
Weights for H_∞ Preview Control Design

Preview Time (s)	Delay States (N)	Gain K
0	0	3.850
0.10	4	3.250
0.20	8	2.700
0.30	12	2.100
0.40	16	1.500
0.50	20	1.000
0.60	24	0.500
0.70	28	0.035
0.80	32	0.041
≥ 0.80	≥ 32	0.041

TABLE IV
Values of gain K used in actuator penalty weight W_{act}

The state matrix and output matrices have the block partitioned form:

$$A = \begin{bmatrix} 0_5 & I_5 \\ A_{21} & A_{22}\end{bmatrix}$$

$$B = \begin{bmatrix} 0_{5\times2} \\ B_1 \end{bmatrix}$$

$$C = \begin{bmatrix} C_1 & C_2 \end{bmatrix}$$

The system matrices are given by:

$$A_{21} = \begin{bmatrix} -34.76 & -0.0616 & 4.709 & 0.2444 & -1.483 \\ -0.7381 & -0.0016 & 2.431 & -0.0007 & -0.0304 \\ 72.79 & 0.0822 & -238.7 & -0.697 & 2.370 \\ 6.918 & -10.54 & -1.269 & -186.5 & -13.32 \\ -49.13 & -8.738 & 5.088 & 13.98 & -188.5 \end{bmatrix}$$

$$A_{22} = \begin{bmatrix} -0.1006 & -0.0605 & 0.0049 & 0.0023 & 0.0106 \\ -0.0125 & -0.0781 & 0.013 & -0.0001 & 0.0014 \\ -6.375 & -19.58 & -3.680 & 0.0264 & 0.0095 \\ 10.74 & 0.0979 & 0.0567 & -3.518 & -7.765 \\ 5.404 & -0.511 & 0.0997 & 7.765 & -3.501 \end{bmatrix}$$

$$B_1 = \begin{bmatrix} 0.0775 & -2.1115 \\ 0.0118 & 1.1015 \\ 6.0254 & -405.343 \\ -0.0254 & 29.4093 \\ -0.7780 & 11.8315 \end{bmatrix}$$

$$C_1 = \begin{bmatrix} 192.5 & 0.389 & 900 & -1.24 & 9.04 \\ 58220 & 50.81 & -211 & -153.5 & 1173 \\ 0 & 0 & 0 & 0 & 0 \end{bmatrix}$$

$$C_2 = \begin{bmatrix} -7.58 & -9.18 & 0.383 & -0.0006 & -0.099 \\ 24.92 & -3.42 & -0.447 & -1.520 & -6.969 \\ 0 & 9.55 & 0 & 0 & 0 \end{bmatrix}$$

$$D = \begin{bmatrix} 7.8878 & -219.6507 \\ -3.7719 & 102.9489 \\ 0 & 0 \end{bmatrix}$$

ACKNOWLEDGMENT

The authors would like to thank A. Wright from the National Renewable Energy Laboratory for providing the CART3 model data. The authors would also like thank Benjamin Sanderse from the Energy Research Centre of the Netherlands for the photo of the CART3.

This work was supported by the University of Minnesota Institute for Renewable Energy and the Environment under Project No. RL-0010-12 entitled "Design Tools for Multivariable Control of Large Wind Turbines."

REFERENCES

[1] T. Burton, D. Sharpe, N. Jenkins, and E. Bossanyi, *Wind Energy Handbook*. Wiley, 2001.

[2] L. Pao and K. Johnson, "Control of wind turbines: Approaches, challenges and recent developments," *IEEE Control Systems Magazine*, vol. 31, no. 2, pp. 44–62, 2011.

[3] J. Laks, L. Pao, and A. Wright, "Combined Feed-forward/Feedback Control of Wind Turbines to Reduce Blade Flap Bending Moments," in *47th AIAA Aerospace Sciences Meeting*, no. AIAA-2009-687, 2009.

[4] J. Laks, L. Pao, A. Wright, N. Kelley, and B. Jonkman, "Blade pitch control with preview wind measurements," in *48th AIAA Aerospace Sciences Meeting and Exhibit*, no. AIAA-2010-251, 2010.

[5] J. Laks, L. Y. Pao, E. Simley, A. Wright, and N. Kelley, "Model predictive control using preview measurements from LIDAR," in *49th AIAA Aerospace Sciences Meeting*, no. AIAA-2011-813, 2011.

[6] A. Korber and R. King, "Nonlinear model predictive control for wind turbines," in *Proceedings of the 2011 EWEA Annual event*, 2011.

[7] M. Soltani, R. Wisniewski, P. Brath, and S. Boyd, "Load reduction of wind turbines using receding horizon control," in *IEEE International Conference on Control Applications*, 2011, pp. 852 –857.

[8] F. Dunne, L. Y. Pao, A. D. Wright, B. Jonkman, N. Kelley, and E. Simley, "Adding feedforward blade pitch control for load mitigation in wind turbines: Non-causal series expansion, preview control, and optimized FIR filter methods," in *49th AIAA Aerospace Sciences Meeting*, no. AIAA-2011-819, 2011.

[9] P. Seiler, A. A. Ozdemir, and G. J. Balas, "Performance limits with preview information and actuator rate constraints," in *American Control Conference*, 2012.

[10] A. Ozdemir, P. Seiler, and G. Balas, "Fundamental limitations of preview for wind turbine control," in *50th AIAA Aerospace Sciences Meeting and Exhibit*, 2012.

[11] B. Jonkman, *TurbSim User's Guide*, National Renewable Energy Laboratory, Golden, Colorado, 2009.

[12] A. Wright, "CART3 FAST model," Personal communication, 2011.

[13] J. M. Jonkman and J. M. L. Buhl, *FAST User's Guide*, National Renewable Energy Laboratory, Golden, Colorado, 2005.

[14] M. Buhl Jr and A. Manjock, "A comparison of wind turbine aeroelastic codes used for certification," in *44th AIAA Aerospace Sciences Meeting and Exhibit*, no. AIAA-2006-786, 2006.

[15] ZephIR Ltd., "ZephIR technical specification," http://www.yourwindlidar.com/technical-specification-zephir, accessed: 09/30/2012.

[16] E. Simley, L. Pao, R. Frehlich, B. Jonkman, and N. Kelley, "Analysis of wind speed measurements using continuous wave lidar for wind turbine control," in *49th AIAA Aerospace Sciences Meeting and Exhibit*, no. AIAA-2011-263, 2011.

[17] R. B. Stull, *An introduction to boundary layer meteorology*. Springer, 1988.

[18] K. A. Stol, "Dynamics modeling and periodic control of horizontal-axis wind turbines," Ph.D. dissertation, University of Colorado at Boulder, Boulder, Colorado, 2001.

[19] K. A. Stol, H.-G. Moll, G. Bir, and H. Namik, "A comparison of multi-blade coordinate transformation and direct periodic techniques for wind turbine control design," in *Proceedings of the 47th AIAA/ASME*, no. AIAA-2009-479, Orlando, Florida, 2009.

[20] W. Johnson, *Helicopter Theory*, 1st ed. Princeton University Press, 1980.

[21] G. Bir, "Multi-blade coordinate transformation and its applications to wind turbine analysis," in *AIAA Wind Energy Symposium*, no. AIAA-2008-1300, Reno, Nevada, 2008.

[22] A. Ozdemir, P. Seiler, and G. Balas, "Performance of disturbance augmented control design in turbulent wind conditions," *Mechatronics*, 2011.

Ahmet Arda Ozdemir Ahmet Arda Ozdemir is a Ph.D. candidate in the Aerospace Engineering and Mechanics Department of the University of Minnesota. He received a B.S. degree in Electrical Engineering from Istanbul Technical University, Turkey in 2008 and a M.S. degree in Aerospace Engineering from University of Minnesota in 2010. His research interests include fault detection and isolation, control modeling, analysis, and synthesis of wind turbines. He is particularly interested in applying physically motivated, low-order models to the control and fault detection design problems.

Peter Seiler Peter Seiler is an Assistant Professor in the Department of Aerospace Engineering and Mechanics at the University of Minnesota. Dr. Seiler previously worked at the Honeywell on various aerospace and automotive applications including the redundancy management system for the Boeing 787, sensor fusion algorithms for automotive active safety systems and re-entry flight control laws for NASA's Orion vehicle. His current research interests include model-based fault-detection and robust control techniques with applications to unmanned aerial vehicles and wind energy. Dr. Seiler is the recipient of the American Automatic Control Council O Hugo Schuck Best Paper Award in 2002.

Gary J. Balas Gary Balas is Head of Aerospace Engineering and Mechanics and Distinguished University McKnight Professor at the University of Minnesota. His research interests include robust control of aerospace systems, real-time control, control of safety critical systems and theoretical control analysis and design tools and techniques. He has received several awards and fellowships including the American Automatic Control Council O Hugo Schuck Best Paper Award in 2006, and the 2005 IEEE Control System Society Control Systems Technology Award. Balas is President of MUSYN Inc., co-developer of the Robust Control Matlab Toolbox, a Fellow of IEEE, and Associate Fellow of AIAA.